O_2 dissociation in Ar–O_2 surface-wave microwave discharges

2012 J. Phys. D: Appl. Phys. 45 195205

(http://iopscience.iop.org/0022-3727/45/19/195205)

IOP PUBLISHING JOURNAL OF PHYSICS D: APPLIED PHYSICS

J. Phys. D: Appl. Phys. **45** (2012) 195205 (8pp) doi:10.1088/0022-3727/45/19/195205

O_2 dissociation in Ar–O_2 surface-wave microwave discharges

Kinga Kutasi[1], Paulo A Sá[2,3] and Vasco Guerra[2]

[1] Research Institute for Solid State Physics and Optics, Hungarian Academy of Sciences, POB 49, H-1525 Budapest, Hungary
[2] Instituto de Plasmas e Fusão Nuclear, Instituto Superior Técnico, Universidade Técnica de Lisboa, 1049-001 Lisboa, Portugal
[3] Departamento de Engenharia Física, Faculdade de Engenharia da Universidade do Porto, 4200-465 Porto, Portugal

E-mail: kutasi@sunserv.kfki.hu

Received 26 September 2011, in final form 29 March 2012
Published 25 April 2012
Online at stacks.iop.org/JPhysD/45/195205

Abstract

A self-consistent model is developed in order to investigate the dissociation of O_2 molecules in Ar–O_2 surface-wave microwave discharges. The dissociation degree of O_2 molecules ($[O]/2[O_2]_0$) is determined for surface-wave discharges generated in 0.5 cm and 2.8 cm diameter tubes with 2.45 GHz and 915 MHz microwave field frequencies, respectively, in the 0.5–25 mbar pressure range at different mixture compositions from pure O_2 to 95%Ar–5%O_2. The dissociation degree varies non-monotonically with pressure—it passes through a minimum—which is more pronounced in high Ar content mixtures. This behaviour is found to be a consequence of the electron collision processes, in particular the evolution of the non-Maxwellian shape of the electron energy distribution function with pressure. These changes make the electron impact dissociation coefficient follow the same non-monotonic trend with pressure, despite leading to the expected monotonic variation of the ionization rate coefficient. The minimum in dissociation is in correlation with the momentum transfer cross-section profiles of the mixture's components, and occurs approximately at the pressure that satisfies the condition $\nu_{ce} = \omega$, which explains its dependence on ω.

(Some figures may appear in colour only in the online journal)

1. Introduction

Afterglow systems based on oxygen containing surface-wave microwave discharges meet several applications in the fields of biomedicine [1–4] and surface treatment [5, 6], with further potential in areas such as nanotechnology [7–9]. In numerous applications the major role is played by the O-atoms; however, most of the time a synergetic effect between the O-atoms and ions or UV photons is observed. For example in the removal of biological contaminants/etching of hydrocarbons the crucial process is the chemical sputtering induced by the Ar^+ ions and O-atoms [10], while in the bacterial inactivation [3, 11, 12] and etching of polyolefins (hexatriacontane—HTC) [5] the synergetic effect between the O-atoms and the VUV/UV radiation, which can originate e.g. from Ar(4s), has been found. Therefore, it is important to understand the formation of O-atoms under different discharge conditions in mixtures which, besides the O-atoms, can also provide the reactive species required by the application processes. The aim of this work is the study of O_2 dissociation in one of the most frequently used mixtures, the Ar–O_2.

The O-atoms density has been determined experimentally by several groups [6, 13–20] in the afterglows of the O_2 and Ar–O_2 surface-wave microwave discharges under selected discharge conditions, in what concerns the gas pressure, mixture composition, field frequency, tube radius and the gas flow. A summary of these measurements can be found in our previous work [9]. Nevertheless, in order to get an insight into the physical and chemical processes that govern the system and to understand the formation of the O-atoms, a systematic study is needed. For this purpose, we conduct theoretical studies on two configurations of surface-wave discharges regarding the generating microwave field frequency and tube radius: (I) $f = 2.45$ GHz and $R = 0.25$ cm [6] and (II) $f = 915$ MHz

Table 1. Creation and destruction processes for oxygen atoms. The rate coefficients for the two- and three-body reactions are in $cm^3\ s^{-1}$ and $cm^6\ s^{-1}$, respectively, while the temperature is measured in K.

Processes	Rate coefficients	Ref.
(R1) $e + O_2(X, a, b) \rightarrow e + O(^3P) + O(^3P)$	$\sigma(\epsilon)$	
(R2) $e + O_2(X, a, b) \rightarrow e + O(^3P) + O(^1D)$	$\sigma(\epsilon)$	
(R3) $e + O_2(X, a) \rightarrow O^- + O(^3P)$	$\sigma(\epsilon)$	
(R4) $e + O_3 \rightarrow e + O(^3P) + O_2(X, 0)$	$\sigma(\epsilon)$	
(R5) $Ar(4s_j) + O_2(X, 0) \rightarrow Ar(^1S_0) + O(^3P) + O(^3P)$	$0.46 \times 2.1 \times 10^{-10}$ [a]	[32, 33]
(R6) $Ar(4s_j) + O_2(X, 0) \rightarrow Ar(^1S_0) + O(^3P) + O(^1D)$	$0.52 \times 2.1 \times 10^{-10}$ [a]	[32, 33]
(R7) $e + O(^3P) \leftrightarrows e + O(^1D)$		
(R8) $Ar(^1S_0) + O(^1D) \rightarrow Ar(^1S_0) + O(^3P)$	3×10^{-13}	[34, 35]
(R9) $O(^3P) + O(^1D) \rightarrow O(^3P) + O(^3P)$	8×10^{-12}	[36]
(R10) $O(^1D) + O_2 \rightarrow O(^3P) + O_2$	$7 \times 10^{-12} \times \exp(67/T)$	[36]
(R11) $O(^1D) + O_2(X) \rightarrow O(^3P) + O_2(a)$	1×10^{-12}	[36]
(R12) $O(^1D) + O_2(X) \rightarrow O(^3P) + O_2(b)$	$2.56 \times 10^{-11} \times \exp(67/T)$	[36]
(R13) $O(^1D) + O_3 \rightarrow O_2(X, 0) + 2O(^3P)$	1.2×10^{-10}	[36]
(R14) $O_2(a) + O_3 \rightarrow O_2(X, 0) + O_2(X, 0) + O(^3P)$	$5.2 \times 10^{-11} \times \exp(-2840/T)$	[27, 36]
(R15) $O_2(b) + O_3 \rightarrow O_2(X, 0) + O_2(X, 0) + O(^3P)$	1.5×10^{-11}	[27, 36]
(R16) $e + O(^3P) \rightarrow e + e + O^+$	$\sigma(\epsilon)$	
(R17) $O(^3P) + O_3 \rightarrow O_2(X, 0) + O_2(X, 0)$	$0.5 \times 1.8 \times 10^{-11} \times \exp(-2300/T)$	[36, 37]
(R18) $O(^3P) + O_3 \rightarrow O_2(a) + O_2(X, 0)$	$0.33 \times 1.8 \times 10^{-11} \times \exp(-2300/T)$	[36, 37]
(R19) $O(^3P) + O_3 \rightarrow O_2(b) + O_2(X, 0)$	$0.17 \times 1.8 \times 10^{-11} \times \exp(-2300/T)$	[36, 37]
(R20) $Ar(^1S_0) + O_2(X, 0) + O(^3P) \rightarrow Ar(^1S_0) + O_3$	$3.9 \times 10^{-34} \times (300/T)^{1.9}$	[34]
(R21) $Ar(^1S_0) + O(^3P) + O(^3P) \rightarrow Ar(^1S_0) + O_2(X, 0)$	$5.2 \times 10^{-35} \times \exp(900/T)$	[34]
(R22) $O(^3P) + O_2(X, 0) + O \rightarrow O_3 + O$	$2.1 \times 10^{-34} \times \exp(345/T)$	[27, 36]
(R23) $O_2 + O_2(X, 0) + O(^3P) \rightarrow O_3 + O_2$	$6.4 \times 10^{-35} \times \exp(663/T)$	[27, 36]
(R24) $O(^3P) + O(^3P) + O_2 \rightarrow O_2 + O_2(X, 0)$	$0.5 \times 3.81 \times 10^{-30} \times \exp(-170/T)/T$	[36, 37]
(R25) $O(^3P) + O(^3P) + O_2 \rightarrow O_2(a) + O_2$	$0.33 \times 3.81 \times 10^{-30} \times \exp(-170/T)/T$	[36, 37]
(R26) $O(^3P) + O(^3P) + O_2 \rightarrow O_2(b) + O_2$	$0.17 \times 3.81 \times 10^{-30} \times \exp(-170/T)/T$	[36, 37]
(R27) $O(^3P) + O(^3P) + O \rightarrow O_2(X, 0) + O$	$3.6 \times 10^{-32} \times (1/T)^{0.63}$	[38]
(R28) $O(^3P) + O_2 + O_3 \rightarrow O_3 + O_3$	$1.66 \times 10^{-34} \times \exp(T/300)$	[34]
(R29) $O(^3P) + \text{wall} \rightarrow 1/2O_2(X, 0)$		
(R30) $O(^1D) + \text{wall} \rightarrow O(^3P)$		

[a] 2.4 instead of 2.1 for the $Ar(^3P_0)$ state.

and $R = 1.25$ cm [1], in a wide range of pressure and mixture compositions. The investigations are carried out with a zero-dimensional kinetic model presented in the next section. Preliminary results have been presented at the 30th International Conference on Phenomena in Ionized Gases [21].

2. Model

The kinetic model is based on the solutions of the steady-state, homogeneous electron Boltzmann equation written for the case of a microwave field, coupled to a system of rate-balance equations for the neutral and charged heavy species. A detailed description of the model is given in our previous works [9, 22]. The validity of the model has been established in those works by comparing the calculated species densities with the available experimental measurements, for different gas mixtures and operating conditions. A short overview of the model is given below.

The steady-state, homogeneous electron Boltzmann equation is solved in an Ar–O_2 mixture, using the two-term expansion in spherical harmonics. It takes into account elastic and inelastic collisions, electron–electron collisions, superelastic collisions producing electronic and vibrational de-excitation, electron dissociation of ground state and excited molecules, and direct and stepwise ionization. Note that elastic, inelastic and ionizing collisions with O-atoms are also included, due to the high degrees of dissociation found in these discharges. The cross section data for oxygen species can be found in [23], and those for Ar species in [24]. The mathematical techniques used for solving the Boltzmann equation for the case of a microwave field are detailed in [25, 26].

The continuity and transport equations for the electrons, different positive ions, and O^- ions are also solved, in order to describe the charged particle motion to the wall under the presence of the radial space-charge field [27]. The reduced sustaining microwave field for the plasma in a cylindrical tube, E/N, is determined using the requirement that, under steady-state conditions, the total rate of ionization must compensate exactly for the rate of electron loss by coupled diffusion to the wall plus electron–ion recombination, under the assumption of a quasi-neutral discharge.

In what concerns the heavy-particle kinetics, we further couple the rate-balance equations for the most important neutral and charged argon and oxygen species, namely: $Ar(^1S_0, {}^3P_2, {}^3P_1, {}^3P_0, {}^1P_1)$, $O_2(X\,{}^3\Sigma_g^-, v)$, $O_2(a\,{}^1\Delta_g, b\,{}^1\Sigma_g^+)$, $O(^3P, {}^1D)$, O_3, Ar^+, Ar_2^+, O_2^+, O^+ and O^-. The collisional–radiative module that describes the excitation and de-excitation of the $3p^5 4s$ levels in a pure Ar discharge has been developed according to the collisional–radiative model of Ferreira *et al* [28, 29]. The processes that contribute to the creation and destruction of oxygen atoms are presented in table 1. The

full list of gas phase and surface reactions—in total 79—taken into account can be found in [22], as well as the corresponding probabilities and rate coefficients.

The plasma generated and sustained with surface wave in a small diameter tube is a plasma column with the electron density decreasing from the launcher to the end of the column, as discussed in [30, 31]. At the end of the plasma column the electron density reaches the value n_{ec}, the critical density for surface-wave mode propagation in a homogeneous, cold, collisionless plasma, surrounded by a dielectric of permittivity ϵ_g. The surface-wave mode can only propagate provided the electron density is larger than this critical value, obtained from $\omega_{pe} > \omega\sqrt{1+\epsilon_g}$, with ω_{pe} denoting the electron plasma angular frequency, which for a quartz tube ($\epsilon_g = 4$) gives $n_{ec} = 3.74 \times 10^{11}\,\mathrm{cm}^{-3}$ and $5.19 \times 10^{10}\,\mathrm{cm}^{-3}$ at 2.45 GHz and 915 MHz, respectively. The calculations are conducted for this critical electron density, so the discharge characteristics are obtained at the end of the plasma column.

3. Results and discussion

The calculations have been carried out in the 0.5–25 mbar pressure range, in mixtures from pure O_2 to 95%Ar–5%O_2. The surface recombination probability of O-atoms, which strongly influences the O-atoms density, has been chosen $\gamma_{O(^3P)} = 8 \times 10^{-3}$ in accordance with the measurements of Macko *et al* [39], while the gas temperature has been fixed to 500 K [9, 31].

3.1. O_2 dissociation degree in a discharge generated with 2.45 GHz frequency field in a $R = 0.25$ cm tube

3.1.1. Dissociation degree and electron collision processes. The dissociation degree of O_2 molecules is defined as $[O]/2[O_2]_0$, where $[O_2]_0$ is the initial density of O_2 in the mixture. The calculated O_2 dissociation degree is shown in figure 1(*a*) as a function of pressure, for different initial mixture compositions. According to the calculations, the highest dissociation degree occurs in the higher Ar content mixture and it exhibits a different pressure dependence with the mixture composition. In the high Ar content mixture discharges the dissociation degree shows a well defined minimum at around 4 mbar. However, with decreasing Ar percentage the minimum becomes less pronounced, and in pure O_2 only a slight increase in the dissociation degree can be observed at $p > 8$ mbar.

The dissociation of the molecules in the discharge is influenced by the electron collisions, as well as by the chemical kinetics of the system. The electron dissociation rates calculated for the different mixture compositions, here presented for the 90%Ar, 50%Ar and 100%O_2 mixtures, figure 1(*b*), exhibit a very similar behaviour with pressure as the dissociation degree. The electron induced dissociation processes—(R1)–(R3) involving both ground and excited state O_2 molecules—have been found to be the dominant sources of O-atoms. Nevertheless, the O-atoms' density is also influenced by the volume and surface loss processes (discussed in section 3.1.3), which induce the differences in shape between the dissociation rates and the dissociation degrees.

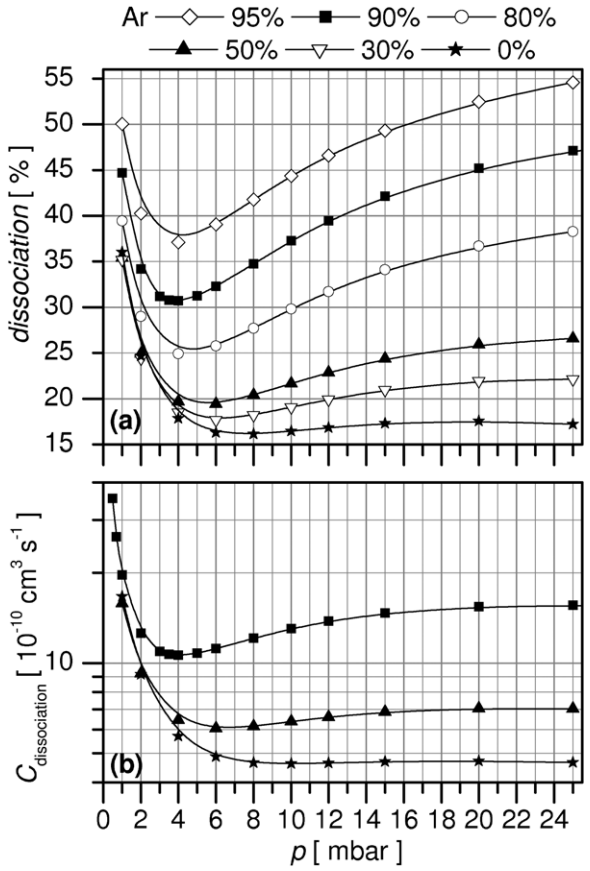

Figure 1. (*a*) O_2 dissociation degree and (*b*) electron dissociation rates as a function of pressure for an Ar–O_2 surface-wave discharge generated in $R = 0.25$ cm with 2.45 GHz.

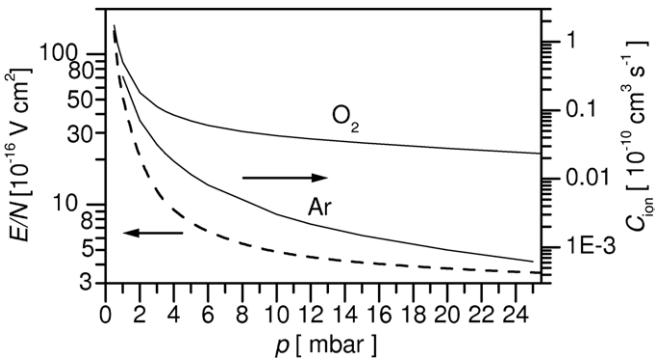

Figure 2. Reduced sustaining field (left axis) and electron ionization rates (right axis) as a function of pressure for a 2.45 GHz surface-wave discharge generated in 90%Ar mixture.

In order to fully understand the results presented in figure 1, in particular the non-monotonic behaviour of both the electron dissociation rate coefficient and the dissociation degree, it is pertinent to look as well at the electron impact ionization rate and the reduced sustaining electric field E/N, N denoting the total gas density. They are represented in figure 2 for the case of a 90%Ar mixture, which shows that the ionization rate and the reduced sustaining field follow the expected monotonic behaviour with pressure, even in mixtures with high Ar content.

Figures 1 and 2 reveal that a global justification for the variation of the electron impact rate coefficients does not

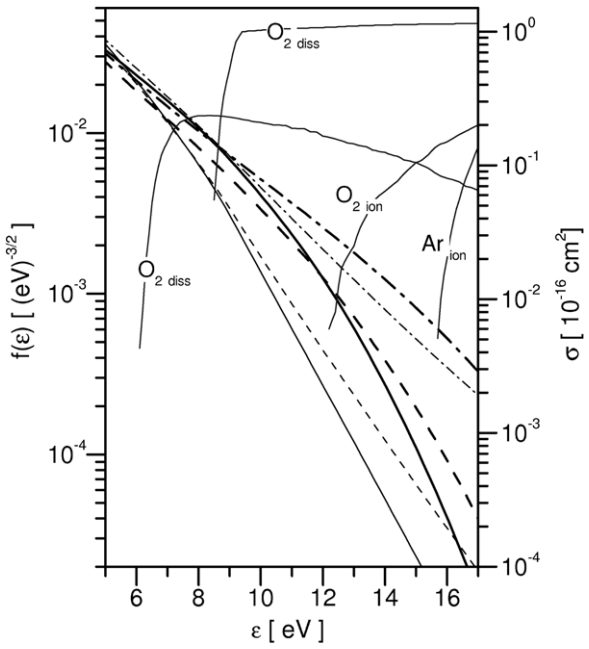

Figure 3. Electron energy distribution function (left axis) at different pressures: 1 mbar (— · —), 4 mbar (- - - -) and 8 mbar (——) in the case of 90%Ar (thick lines) and 0%Ar (100%O_2) (thin lines) calculated for the microwave field of 2.45 GHz frequency; and collision cross sections (right axis) [40, 41, 43].

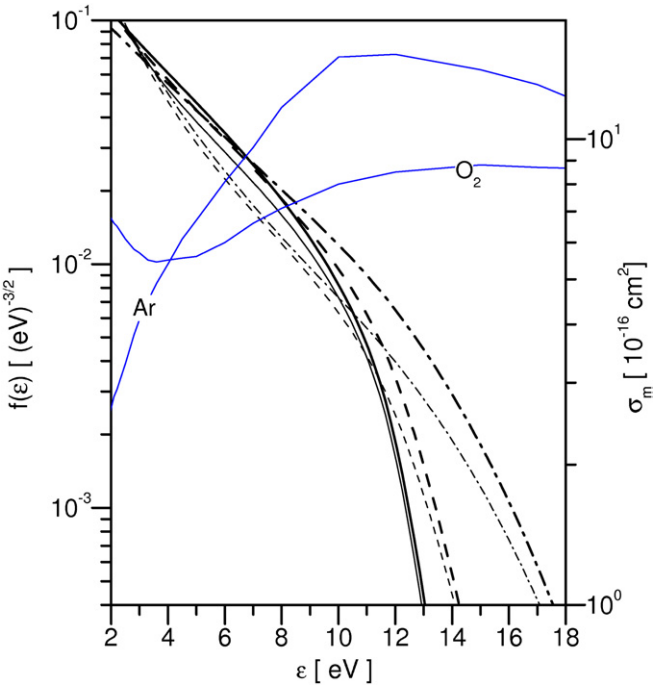

Figure 4. EEDF (left axis) at different pressures: 1 mbar (— · —), 4 mbar (- - - -) and 8 mbar (——) in 100%Ar calculated with σ_m (thin lines) and with constant momentum cross-section (thick lines, see text); and momentum cross-sections (right axis) [40, 41, 43].

exist. Instead, a detailed explanation must rest on the shapes of the electron energy distribution function (EEDF) and of the relevant cross-sections, as processes with different energy threshold manifest a different response to pressure variations. Figure 3 depicts the calculated EEDFs at different pressures and for two mixture compositions, together with the cross-sections of the processes under analysis. As can be seen, the deviation of the EEDF from a Maxwellian increases with the Ar content in the mixture. An overpopulation of the EEDF in the 6–12 eV energy range occurs in high Ar content mixtures—but not in pure O_2—as the pressure raises above 4 mbar. This energy region corresponds to the group of electrons that are able to dissociate O_2 molecules, as shown by the collision cross-section presented in the figure. We note that the 6.0 eV loss corresponds to the excitation of the pre-dissociative levels of $C\,^3\Delta_u$, $A\,^3\Sigma_u^+$ and $c\,^1\Sigma_u^-$ leading to dissociation forming two O(^{3}P) atoms, while the 8.4 eV loss corresponds to the dissociative excitation of $B\,^3\Sigma_u^-$, forming O(^{3}P) and O(^{1}D). Due to this overpopulation a similar behaviour is observed for other electron excitation rates. However, this is not the case for the ionization rates, which have high energy thresholds.

A deeper understanding of the origin of the different behaviour with pressure of groups of electrons with different energies seen in figure 3 can be achieved with two additional remarks. First is to note that in high-frequency discharges the EEDF is a function of the two independent parameters, E/N and ω/N [25], which decrease with pressure. But whereas the former effect leads to a diminution of the electron impact rate coefficients, the latter leads to their increase [25]. In principle, a non-monotonic behaviour of the dissociation rate coefficient shown in figure 1 may arise as a result of the competition between these two opposing effects. However, the actual behaviour depends on the particular shape of the cross-sections, as the different results obtained for the ionization coefficient strikingly demonstrate. The second noteworthy observation is that, for our conditions, the overpopulation in the 6–12 eV region has been found to be a consequence of the markedly increasing profile of the Ar momentum transfer cross-section (σ_m) for electron energies from the Ramsauer minimum (∼0.2 eV) up to 12 eV. As a matter of fact, the calculations conducted in pure Ar by imposing a constant σ_m have shown that the overpopulation previously observed vanishes, as illustrated in figure 4, where the calculations have been conducted by choosing the maximum value of the actual cross-section. Simulations performed by taking other constant values of σ_m, such as the average value in this energy range, lead to similar results. Furthermore, in the case of a constant Ar σ_m the dissociation degree exhibits a similar behaviour with pressure in a 90%Ar mixture to the one obtained in pure O_2, which definitely substantiates this interpretation.

3.1.2. Prediction of the dissociation degree behaviour based on electron collision frequencies. The momentum transfer cross-section σ_m—that defines the momentum transfer collision frequency—also determines the power gain of electrons with energy ε from the external field, given by the relation

$$\nu_c\ \varepsilon = \frac{(eE)^2 \nu_c}{2m(\nu_c^2 + \omega^2)}, \qquad (1)$$

where $\nu_c(\varepsilon)$ and ω are the electron collision and field frequencies, respectively, E is the sustaining field [42] and e and m are the absolute value of the electron charge and the

electron mass, respectively. The power gain is maximum when $\nu_c = \omega$.

Raizer [42] has observed a similar behaviour to that of the dissociation degree for the breakdown threshold field in the case of laser induced discharges, where the positions of the minima along the pressure scale corresponded to the approximate equality of the angular frequency of light and the collision frequency (the collision frequency has been taken electron energy independent), which is the condition of the maximum power gain. In order to verify if the dissociation degree's behaviour is linked to a similar effect we proceed with the analysis of the collision and field frequencies.

For the present estimation purposes—to compare ν_c with ω—ν_c is taken here as the effective collision frequency, ν_{ce} as defined in [44, 46]. In our case, we consider the values $\nu_{ce}(\mathrm{Ar})/N = 2.0 \times 10^{-7}\,\mathrm{cm^3\,s^{-1}}$ [44] and $\nu_{ce}(\mathrm{O_2})/N = 1.3 \times 10^{-7}\,\mathrm{cm^3\,s^{-1}}$ [13, 47], which ensure that the ionization coefficient can be expressed as a unique function of the reduced effective field for all ω/ν_{ce} [44, 46]. Take note that for a mixture with a fraction of Ar δ, the effective collision frequency is obtained from $\nu_{ce} = \delta\nu_{ce}(\mathrm{Ar}) + (1-\delta)\nu_{ce}(\mathrm{O_2})$.

To clarify the origin of ν_{ce} we make the following remarks. In the case of the alternating fields, such as in a microwave discharge, the effective field approximation [44] can be used whenever $\omega \gg \nu_e$, where ν_e is the energy relaxation frequency. In this case, the time modulation of the EEDF is strongly reduced [44]. Moreover, if the (effective) collision frequency for momentum transfer ν_c, which may include both elastic and inelastic contributions [45], is independent of the electron energy, the EEDF can be obtained by solving the Boltzmann equation in a dc field, with an effective field strength given by $E_{\mathrm{eff}} = (E_0/\sqrt{2})\nu_c^2/(\omega^2+\nu_c^2)^2$. The effective field approximation has been extended to situations where ν_c depends on the electron energy by replacing $\nu_c(u)$ by a momentum transfer collision frequency for the bulk electrons ν_{ce} which can be somewhat arbitrarily chosen, provided it is verified that it leads to a correct calculation of the transport parameters [44, 46]. In this case, the Boltzmann equation can be solved as in a dc field replacing E by E_{eff}.

Figure 5 shows the effective collision and the field frequencies as a function of pressure, together with the dissociation degree for the 90%Ar and pure O_2 mixtures. It can be observed that the minimum of the dissociation degree occurs close to the condition of the $\nu_{ce} = \omega$, which implies maximum energy gain for the electron. When the energy gain of the electron from the external field during one cycle is maximum, the electron is able to acquire high energy that can be, and is more likely to be, consumed for ionization (that can also lead to a minimum breakdown field observed by Raizer [42]), instead of lower threshold excitations and dissociations. In the case of low energy gains the electrons loose their energy in excitation processes and have difficulty reaching the ionization threshold (which can lead to the increase in the breakdown field). This could explain the minimum of the dissociation at the condition of the maximum energy gain. This effect is more pronounced in molecular gas—atomic gas mixtures, in particular in atomic gas dominant mixtures, since the gas atoms have much higher ionization thresholds than the molecules.

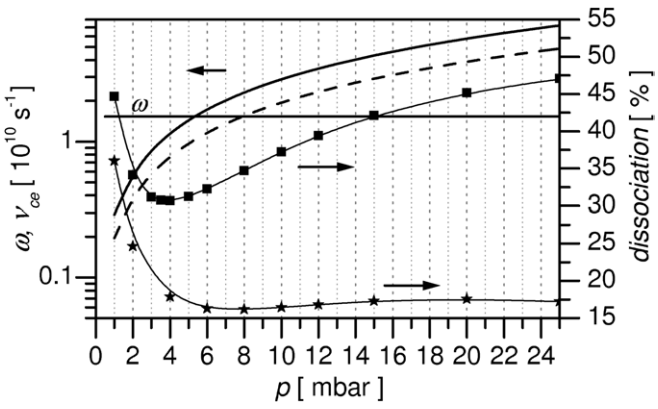

Figure 5. Field and electron collision frequencies (left axis) and dissociation degree (right axis) as a function of pressure in the case of 90%Ar (—— and ■) and 0%Ar (- - - - and ⋆) discharges.

Here it is more difficult for electrons to reach the ionization potential since they are decelerated due to the molecular excitation and dissociation processes.

3.1.3. Dissociation degree and the chemical kinetics. As already mentioned, the dissociation degree of O_2 is also influenced by the chemical kinetics since, in addition to electron impact collisions, both the O_2 and O densities are also determined by the volume and surface reactions (see table 1). In high Ar content mixtures the collisions of Ar(4s) atoms with O_2 can contribute to the O_2 dissociation ((R5)–(R6) from table 1), at 1 mbar in a 95%Ar mixture with about 14%, which decreases to about 3% at 25 mbar, and overall decreases with Ar percentage. In what concerns the O-atoms, with increasing O_2 percentage in the mixture the three-body recombination of O-atoms ((R24)–(R26)) starts to play a role at pressures higher than 10 mbar: in the case of a 50%Ar mixture at 25 mbar its contribution to the O(^{3}P) destruction is 4%, while in pure O_2 it is 12%. At the same time the surface recombination of atoms (R29), which is their dominant loss process, becomes less efficient with pressure.

3.1.4. Comparison with experimental results. The dissociation degree at different pressures has been determined experimentally by Mafra *et al* [6] for the 90%Ar–10%O_2 mixture. The microwave discharge has been generated with 2.45 GHz in a 0.5 cm diameter tube having 45 cm length and connected at the end to a 2.8 cm post-discharge tube. The gas flow was set to 1000 sccm. The density of oxygen atoms was determined at the entrance of the larger diameter tube by NO titration using a special mixing device presented in [48], which had the same diameter as the discharge tube. Since the discharge tube is very long, the afterglow already develops in this tube before entering the larger one. The starting position of the afterglow, as well as the afterglow time at a given position depend on the pressure, since the length of the discharge and the gas velocity change with pressure. Thus, the O-atom densities measured at the same system position at different pressures were in fact determined at different instants of the afterglow. As the gas velocity for constant gas flow rate decreases with

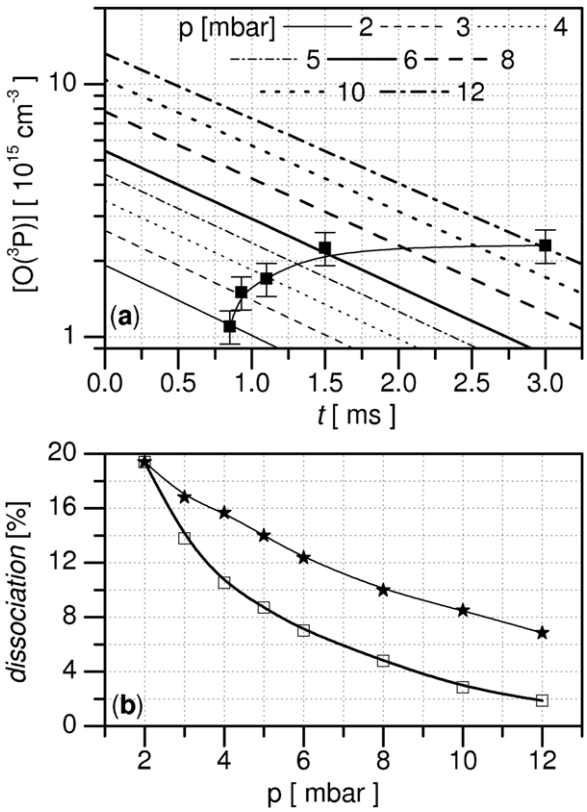

Figure 6. (*a*) Calculated O(^{3}P) densities along the afterglow (lines) and measured O-atoms densities (■) taken from [6], and (*b*) calculated dissociation degrees at afterglow times estimated from the comparison of calculated and experimental densities (⋆), and from the change of gas velocity with pressure (□) (see text) for different pressure values.

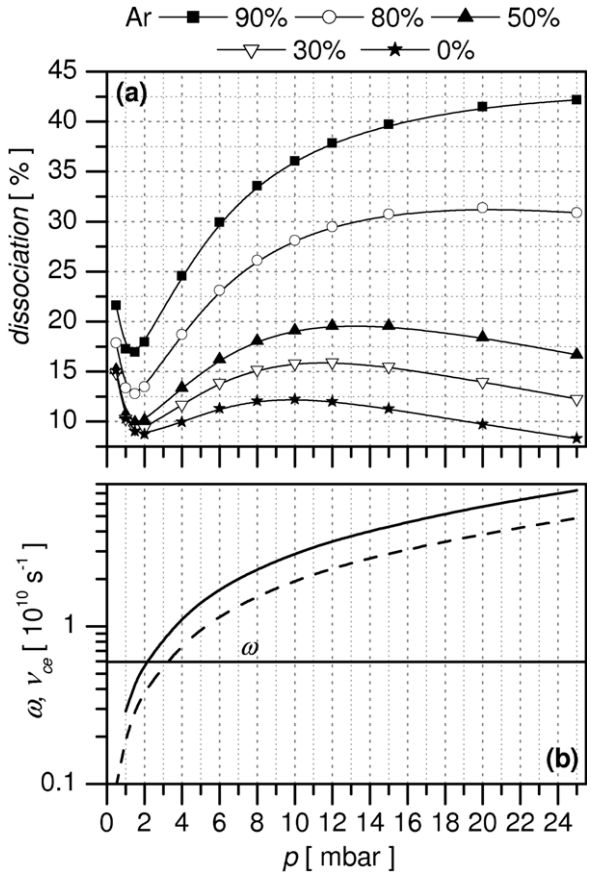

Figure 7. (*a*) O_2 dissociation degree and (*b*) field and electron collision frequencies (90%Ar —— and 0%Ar - - - -) as a function of pressure in an Ar–O_2 surface-wave discharge generated in $R = 1.25$ cm with 915 MHz.

pressure, it is expected that at higher pressures the measured O densities correspond to larger afterglow times.

Figure 6(*a*) shows the calculated O(^{3}P) density along the afterglow at different pressures, as well as the measured O-atoms' density [6] placed on the corresponding pressure curves at the afterglow time where it equals the calculated densities. It can be observed that the difference in afterglow time between the 2 mbar and the 12 mbar cases is about a factor of 4, which is less than the afterglow time difference suggested just by the change of the gas velocity with pressure at otherwise similar conditions, which would give a factor of 6. The so obtained afterglow times are just estimations, not only due to the measurement uncertainties, but also to a possible difference between the surface recombination probabilities used in the model and characteristic for the system [49].

Figure 6(*b*) shows the dissociation degrees calculated at different pressures for the afterglow time suggested by the densities comparison, as well as for afterglow times resulting only from the change of the gas velocity with pressure. These dissociation profiles, which reflect the behaviour of the experimentally determined ones [6], do not show the characteristics exhibited by those determined from densities taken for the same afterglow time at different pressures (see figure 1, and figure 10 in [9]). This shows that the dissociation profiles predicted by the calculations can be verified only in systems which allow the measurement of the densities at the same instant in the afterglow at different pressures, either by changing the position of the measurement or that of the discharge generation.

3.2. O_2 dissociation degree in a discharge generated with 915 MHz frequency field in a $R = 1.4$ cm tube

By choosing a lower field frequency the critical electron density becomes smaller, changing from 3.74×10^{11} cm^{-3} at 2.45 GHz to 5.19×10^{10} cm^{-3} at 915 MHz. At the same time, this smaller field frequency will be equalized by the electron collision frequency at lower pressures than in the case of the 2.45 GHz frequency (referred as case I), which suggest that the minimum in the dissociation degree occurs at lower pressures. Figure 7(*a*) shows the calculated dissociation degrees for different gas mixtures as a function of pressure, while in figure 7(*b*) the collision and field frequencies are represented. The figure shows that the minimum in the dissociation degree is obtained in the 1–3 mbar range, which is close to the condition satisfying $\nu_{ce} = \omega$, as predicted. Furthermore, in this discharge the saturation of the dissociation degree can be observed at lower pressures than in case I. This is a consequence of the increased contribution of gas phase recombination, since the discharge volume is larger than in case I (here $R = 1.4$ cm comparing to 0.25 cm in case I). The calculations reveal that three-body recombination becomes

important at pressures $p \geqslant 6$ mbar. In pure O_2 and at 10 mbar it contributes with about 10% to the $O(^3P)$ destruction, increasing to 44% at 25 mbar. At this later pressure the contribution of three-body reactions to the O-atoms destruction decreases with the Ar content, being of 24% in a 50%Ar mixture, 9% in a 80%Ar mixture, and less than 3% in a 90%Ar mixture.

4. Conclusions

In this work we have studied the dissociation of O_2 molecules in Ar–O_2 surface-wave microwave discharges. We have investigated two surface-wave discharges, that differ in the generating microwave field frequency and tube radius: (I) $f = 2.45$ GHz and $R = 0.25$ cm and (II) $f = 915$ MHz and $R = 1.25$ cm. These discharges have been studied with the zero-dimensional kinetic model, which allows the calculation of the electron energy distribution function (EEDF), the sustaining field and the species densities for a given electron density. The calculations have been conducted for the critical electron density for the surface-wave propagation, which occurs at the end of the plasma column.

We have shown that the dissociation degree of O_2 molecules in an Ar–O_2 surface-wave microwave discharge does not vary monotonically with pressure, but passes through a minimum approximately at a pressure satisfying the condition $\nu_{ce} = \omega$. This condition provides a simple criterion to find the minimum in the O_2 dissociation and explains its dependence on ω. We have further shown that the appearance of the minimum is a result of the electron collision processes and the non-Maxwellian character of the EEDF, being a consequence of the electron energy dependent profile of the momentum transfer cross-sections of the mixture's components.

By comparing the calculation results with the experimental measurements, we have shown that the dissociation degree profiles predicted by the calculations can be obtained experimentally only in systems where the densities at different pressures are measured at the same instants in the afterglow. The afterglow time corresponding to a fixed position varies with pressure due to the modifications in the length of the discharge and in the gas velocity. Therefore, the measurements need to be done at different positions in the afterglow.

Acknowledgments

The work has been supported by the Portuguese FCT funds to Instituto de Plasmas e Fusão Nuclear—Laboratório Associado, by Hungarian TeT_10-1-2011-0717 funds and by János Bolyai Research Scholarship of Hungarian Academy of Sciences. The authors would like to thank Thierry Belmonte for the rewarding discussions

References

[1] Philip N, Saoudi B, Crevier M-C, Moisan M, Barbeau J and Pelletier J 2002 *IEEE Trans. Plasma Sci.* **30** 1429
[2] Villeger S, Cousty S, Ricard A and Sixou M 2003 *J. Phys. D: Appl. Phys.* **36** L60
[3] Boudam M K, Saoudi B, Moisan M and Ricard A 2007 *J. Phys. D: Appl. Phys.* **40** 1694
[4] Kutasi K, Saoudi B, Pintassilgo C D, Loureiro J and Moisan M 2008 *Plasma Process. Polym.* **5** 840
[5] Belmonte T, Pintassilgo C D, Czerwiec T, Henrion G, Hody V, Thiebaut J M and Loureiro J 2005 *Surf. Coat. Technol.* **200** 26
[6] Mafra M, Belmonte T, Poncin-Epaillard F , Maliska A and Cvelbar U 2009 *Plasma Process. Polym.* **6** S198
[7] Mozetič M, Cvelbar U, Sunkara M K and Vaddiraju S 2005 *Adv. Mater.* **17** 2138
[8] Cvelbar U, Ostrikov K and Mozetić M 2008 *Nanotechnology* **19** 405605
[9] Kutasi K, Guerra V and Sá P 2011 *Plasma Sources Sci. Technol.* **20** 035006
[10] Rauscher H, Kylián O, Benedikt J, von Keudell A and Rossi F 2010 *ChemPhysChem* **11** 1382
[11] Stapelmann K, Kylián O, Denis B and Rossi F 2008 *J. Phys. D: Appl. Phys.* **41** 192005
[12] Vicoveanu D, Popescu S, Ohtsu Y and Fujita H 2008 *Plasma Processes Polym.* **5** 350
[13] Granier A, Pasquiers S, Boisse-Laporte C, Darchicourt R, Leprince P and Marec J 1989 *J. Phys. D: Appl. Phys.* **22** 1487
[14] Ricard A, Gaillard M, Monna V, Vesel A and Mozetič M 2001 *Surf. Coat. Technol.* **142-144** 333
[15] Ricard A and Monna V 2002 *Plasma Sources Sci. Technol.* **11** A150
[16] Ricard A, Monna M and Mozetič M 2003 *Surf. Coat. Technol.* **174–175** 905
[17] Czerwiec T, Gavillet J, Belmonte T, Michel H and Ricard A 1998 *Surf. Coat. Technol.* **98** 1411
[18] Mozetič M, Ricard A, Babič D, Poberaj I, Levaton J, Monna V and Cvelbar U 2003 *J. Vac. Sci. Technol.* A **21** 369
[19] Mozetič M, Vesel A, Cvelbar U and Ricard A 2006 *Plasma Chem. Plasma Process.* **26** 103
[20] Canal C, Gabriau F, Ricard A, Mozatić M, Cvelbar U and Drenik A 2007 *Plasma Chem. Plasma Process.* **27** 404
[21] Kutasi K, Guerra V and Sá P A 2011 O_2 dissociation in Ar–O_2 surface-wave microwave discharges *30th Int. Conf. on Phenomena in Ionized Gases (ICPIG) (Belfast, Northern Ireland, 28 August–2 September 2011)* C9-282
[22] Kutasi K, Guerra V and Sá P 2010 *J. Phys. D: Appl. Phys.* **43** 175201
[23] Gousset G, Ferreira C M, Pinheiro M, Sá P A, Touzeau M, Vialle M and Loureiro J 1991 *J. Phys. D: Appl. Phys.* **24** 290
[24] Ferreira C M and Loureiro J 1983 *J. Phys. D: Appl. Phys.* **16** 1611
[25] Ferreira C M and Loureiro J 2000 *Plasma Sources Sci. Technol.* **9** 528
[26] Ferreira C M and Loureiro J 1989 *J. Phys. D: Appl. Phys.* **22** 76
[27] Guerra V and Loureiro J 1999 *Plasma Sources Sci. Technol.* **8** 110
[28] Sá P, Loureiro J and Ferreira C M 1992 *J. Phys. D: Appl. Phys.* **25** 960
[29] Ferreira C M, Loureiro J and Ricard A 1985 *J. Appl. Phys.* **57** 82
[30] Moisan M and Zakrzewski Z 1991 *J. Phys. D: Appl. Phys.* **24** 1025
[31] Tatarova E, Dias F M, Ferreira C M and Ricard A 1999 *J. Appl. Phys.* **85** 49
[32] Piper L G, Velazco J E and D. W. Setser 1973 *J. Chem. Phys.* **59** 3323
[33] Balamuta J and Golde M F 1982 *J. Phys. Chem.* **86** 2765
[34] Belmonte T, Czerwiec T, Gavillet J and Michel H 1997 *Surf. Coat. Technol.* **97** 642
[35] Sato T and Makabe T 2008 *J. Phys. D: Appl. Phys.* **41** 035211
[36] Eliasson B and Kogelschatz U 1986 *Brown Boveri Forschungszentrum Report KLR 86-11 C*

[37] Feoktistov V A, Mukhovatova A V, Popov A M and Rakhimova T V 1995 *J. Phys. D: Appl. Phys.* **28** 1346
[38] Gordiets B, Ferreira C M, Guerra V, Loureiro J, Nahorny J, Pagnon D, Touzeau M and Vialle M 1995 *IEEE Trans. Plasma Sci.* **23** 750
[39] Macko P, Veis P and Cernogora G S 2004 *Plasma Sources Sci. Technol.* **13** 251
[40] Lawton S A and Phelps A V 1978 *J. Chem. Phys.* **69** 1055
[41] Phelps A V and Pitchford L 1985 *Phys. Rev.* A **31** 2932
[42] Raizer Yu P 1977 *Laser-Induced Discharge Phenomena* (*Studies in Soviet Science. Physical Sciences*) (New York: Consultants Bureau)
Raizer Yu P 1980 *Sov. Phys.—Usp.* **23** 789
[43] Yamabe C, Buckman S J and Phelps A V 1983 *Phys. Rev.* A **27** 1345
[44] Ferreira C M and Loureiro J 1984 *J. Phys. D: Appl. Phys.* **17** 1175
[45] Pitchford L C and Phelps A V 1982 *Phys. Rev.* A **25** 540
[46] Ferreira C M and Moisan M 1988 *Phys. Scr.* **38** 382
[47] Pinheiro M J 1993 *PhD Thesis* Technical University of Lisbon (in Portuguese)
[48] Bernardelli E A, Ricard A and Belmonte T 2011 *Plasma Sources Sci. Technol.* **20** 025012
[49] Kutasi K and Loureiro J 2007 *J. Phys. D: Appl. Phys.* **40** 5612